Research Journal of Applied Sciences, Engineering and Technology 4(6): 557-570, 2012
ISSN: 2040-7467

Submitted: September 21, 2011 Accepted: December 09, 2011 Published: March 15, 2012

Dual Functional Unified Power Quality Conditioner to Power Quality Enhancement and Wind Energy Injection to Grid

M. Najafi, M. Hoseynpoor and R. Ebrahimi
Bushehr Branch, Islamic Azad University, Bushehr, Iran

Abstract: This study proposes a combined operation of the Unified Power Quality Conditioner (UPQC) with wind power generation system considering investment cost. The proposed system consists of a series inverter, a shunt inverter, and an induction generator connected in the dc link through a converter. The proposed system can compensate voltage sag and swell, voltage interruption, harmonics, and reactive power in both interconnected mode and islanding mode. The speed of the induction generator is controlled according to the variation of the wind speed in order to produce the maximum output power. The investment cost of proposed system is compared with investment cost of separated use of UPQC and Wind Energy Conversion System (WECS) and the economic saving due to use of proposed system is estimated. The validity of the proposed system is verified by the results of computer simulation.

Key word: Maximum power point tracking, power quality improvement, series active filter, shunt active filter, unified power quality conditioner, wind energy conversion system

INTRODUCTION

One of the most interesting structures of energy conditioner is two back-to-back connected dc/ac fully controlled converters. In this case, depending on the control scheme, the converters may have different compensation functions. For example, they can function as active series and shunt filters to compensate simultaneously load current harmonics and supply voltage fluctuations. In this case, the equipment is called Unified Power Quality Conditioner (UPQC) (Akagi *et al*., 2007; Aredes and Watanabe, 1995; Cavalcanti *et al*., 2005; Han *et al*., 2006).

An active shunt filter is a suitable device for current-based compensation (Cavalcanti *et al*., 2005). It can compensate current harmonics and reactive power. The active series filter is normally used for voltage harmonics and voltage sags and swells compensation (Cavalcanti *et al*., 2005). The UPQC, which has two inverters that share one dc link capacitor, can compensate the voltage sag and swell, the harmonic current and voltage, and control the power flow and voltage stability. Nevertheless, UPQC cannot compensate the voltage interruption due to lack of energy source in its dc link (Han *et al*., 2006).

Nowadays, generation of electricity from renewable sources has improved very much. Utilizing of wind energy as a renewable source to generate electricity has developed extremely rapidly and many commercial wind generating units are now available on the market. The cost of generating electricity from wind has fallen almost 90% since the 1980s (Karrari *et al*., 2005).

Wind is a variable and random source of energy. All types of machines, i.e., dc, synchronous, induction, depending on the size of the system have been used to convert this form of energy to electrical energy. Induction generators are more common and more economical by improvement of power electronics devices and drive methods (Datta and Rangenathan, 2002).

Various forms of systems can be used to have some level of control on the wind generation unit. In the variable speed constant frequency systems, power electronic devices are used to allow the rotor speed to be changed while the grid frequency is constant. In one scheme, as studied in this paper, a Variable Speed Cage Machine (VSCM) system is used with a rectifier and an inverter connecting the cage induction generator stator to the grid. The advantage of the variable speed constant frequency system is that the rotor speed can be controlled. This makes it possible to capture maximum energy from the wind turbine (Karrari *et al*., 2005). In Datta and Rangenathan (2003), a method of tracking the peak power points for a VSCM system is suggested. Maximizing the penetration of wind generation in distribution networks is discussed in (Weisser and Garcia, 2005). As the rectifier allows the change of the rotor flux, the operator can also maximize the efficiency of the induction generator.

Numerous research papers are now available on UPQC and distributed generation. In Han *et al*. (2006) a new combined UPQC and synchronous generator is proposed, in which the synchronous generator is connected to UPQC DC bus through an uncontrolled rectifier.

Corresponding Auther: M. Najafi, Bushehr Branch, Islamic Azad University, Bushehr, Iran

In this study a new configuration of UPQC is proposed that has a Wind Energy Generation System (WEGS) connected to the dc link through the rectifier as shown in Fig. 1. The significant advantage of this configuration in compare with separate operation of UPQC and wind energy generation system is reduction in using of one inverter and use of shunt inverter of UPQC as a WEGS's inverter. The UPQC can compensate the voltage interruption in the source, while the WEGS supplies power to the source and load or the load only. There are two operation modes in the proposed system. The first is interconnected mode, in which the WEGS provides power to the source and the load. The second is islanding mode, in which the WEGS provides power to the load only within its power rating when voltage interruption occurs. The system operation transfers from the islanding mode to the interconnected mode when the voltage interruption is removed. The VA rating of series and shunt inverters of UPQC are estimated for proposed system. The investment cost of proposed system is compared with investment cost of separated use of UPQC and WECS using the VA rating calculations and the economic saving due to use of proposed system is estimated.

MATERIALS AND METHODS

In Fig. 1, there are six main parts in proposed system: wind turbine, induction generator, maximum power point tracking which controls induction generator speed, PWM rectifier, shunt inverter and series inverter of UPQC. The modeling of each section is discussed separately and then the overall model is investigated.

Wind turbine: The output power from a wind turbine can be expressed as (Kim and Kim, 2007):

$$\lambda = \frac{w_r R}{V_{WIND}} \quad (1)$$

$$P_M = \frac{1}{2}\rho\pi R^2 C_P V_{WIND}^3 \quad (2)$$

$$T_M = \frac{P_M}{\omega_r} = \frac{1}{2}\rho\pi R^5 C_P \frac{\omega_M^3}{\lambda^3} \quad (3)$$

where, λ is tip-speed ratio, V_{WIND} is the wind speed, R is blade radius, ω_r is the rotor speed (in rad/s),*p is the air density, C_p is the power coefficient, P_M is mechanical output power of wind turbine and T_M is the output torque of wind turbine.

The power coefficient C_p depends on the pitch angle β, the angle at which the rotor blades can rotate along its long axis, and tip-speed ratio λ given by (4), (Surgevil and Akpınar, 2005):

$$C_P = (0.44 - 0.0167\beta)\sin\frac{\pi(\lambda - 2)}{13 - 0.3\beta} - 0.00184(\lambda - 2)\beta \quad (4)$$

where, β is the blade pitch angle. For a fixed pitch type, the value of β is set to a constant value.

Maximum power point tracking: In this study, the pitch angle is kept at zero until the nominal power of the induction generator is reached (Horiuchi and Kawahito, 2001). At high wind speeds, the pitch angle is increased to limit the input power.

Therefore, the optimized rotational speed $\acute{\omega}_{opt}$ for maximum aerodynamic efficiency for a given wind velocity is given by:

$$\omega_{opt} = \frac{\lambda_{opt} V_{WIND}}{R} \quad (5)$$

where, λ_{opt} is the optimized tip-speed ratio which β is zero and C_p is maximum. Hence, to fully utilize the wind energy, λ should be maintained at λ_{opt}, which is determined from the blade design (Abo-Khalil *et al*., 2004). Then from (2):

$$P_{M\max} = \frac{1}{2}\rho\pi R^2 C_{P\max} V^3_{WIND} \quad (6)$$

where, P_{Mmax} is maximum mechanical output power of wind turbine at a given wind speed. The Power coefficient factor versus tip-speed ratio for various pitch angles is shown in Fig. 2.

Once the wind velocity V_{WIND} is measured, the reference speed for extracting the maximum point is obtained from (5).

Induction generator: In this study, a fifth order model for induction generator simulation is used. To overcome the complexity of the model, usually Park's transformation is used. The transformed induction machine equations are described in (Ong, 1997). Also, it is shown:

$$\begin{aligned} T_e &= \frac{3}{2}\frac{P}{2\omega_b} x_m (i_{dr} i_{qs} - i_{qr} i_{ds}) \\ &= \frac{3}{2}\frac{P}{2\omega_b}(\psi_{qr} i_{dr} - \psi_{dr} i_{qr}) \end{aligned} \quad (7)$$

$$T_e = \frac{3P}{4}(\lambda_{qr} i_{dr} - \lambda_{dr} i_{qr}) \quad (8)$$

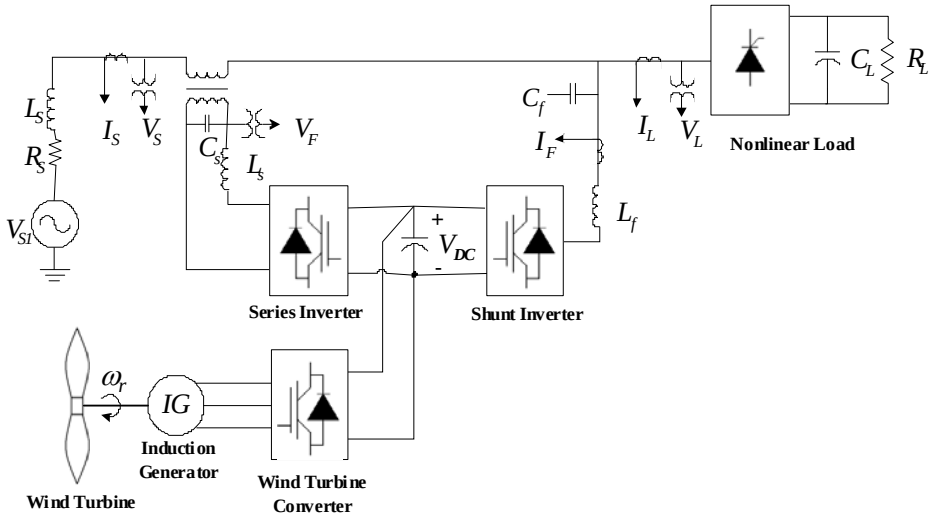

Fig. 1: Configuration of proposed UPQC with WECS

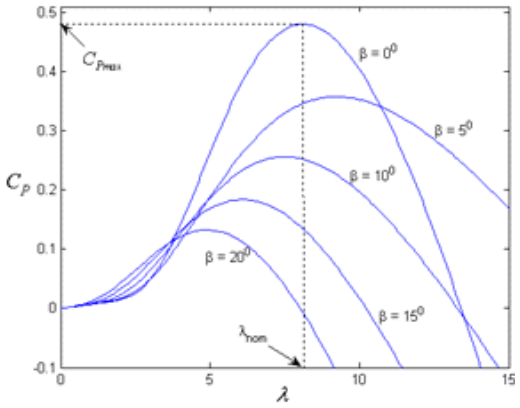

Fig. 2: Power coefficient factor versus tip-speed ratio for various pitch angles

where, P/2 is the number of poles in the induction generator. Equation (8) describes torque equation of an induction generator.

Wind turbine converter: The mechanical output power of wind turbine and rotor speed for a given wind speed is determined by the intersection of wind turbine and the induction generator characteristic curves.

Rotor flux reference frame is used for transformation of induction machine equations. Selecting the d-axis aligned with the rotor flux, the q-axis component of the flux will be zero. This makes the equations easier to handle. In this frame, the torque and flux Eq. (13) described in (8) can be rewritten as:

$$\psi_{qr}\, x_r . i_{qr} + x_m . i_{qs} = 0 \rightarrow \; iqr = -\frac{x_m}{x_r} i_{qs} \qquad (9)$$

$$T_e = -\frac{3P}{4}\lambda_{dr}\, i_{qr} = \frac{3P}{4}\frac{x_m}{x_r}\lambda_{dr}\, i_{qs} \qquad (10)$$

$$\omega - \omega_r = \frac{x_m}{T_r}\frac{i_{qs}}{\lambda_{dr}} \qquad (11)$$

$$\lambda_{dr} = \frac{x_m}{1 + T_r . p} . i_{ds} \qquad (12)$$

where, T_r is time constant of rotor and equals L_r / R_r.

The Eq. (9) to (12), are the basis for field oriented control. This approach simplifies the induction machine control. The model is very similar to a separately excited dc machine where the flux depends on the field current

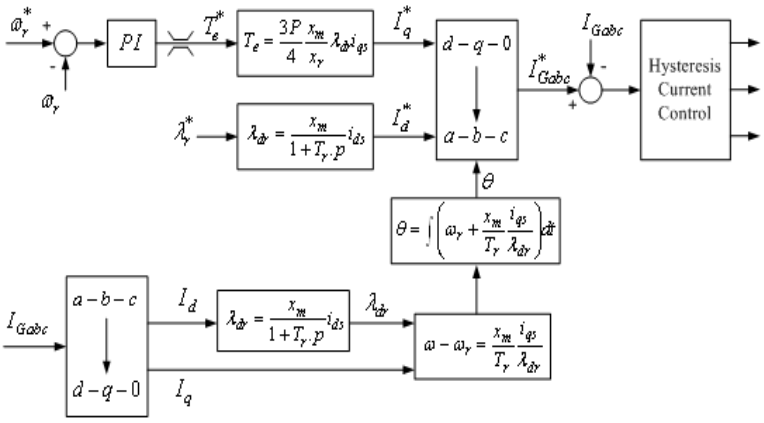

Fig. 3: Wind turbine converter control block diagram

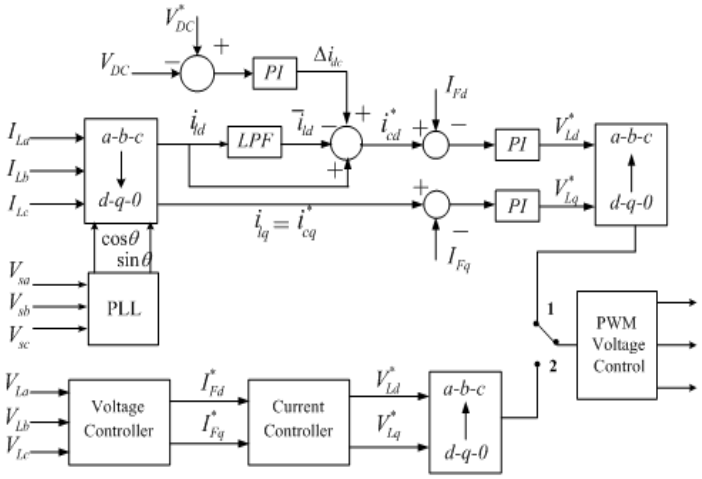

Fig. 4: Shunt inverter control block diagram

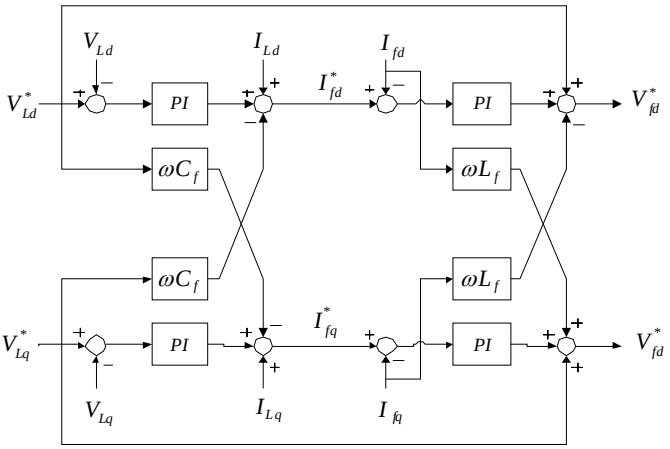

Fig. 5: voltage control of shunt inverter of UPQC in interruption mode

and the torque is proportional to the flux and the armature current. The main problem associated with field oriented control is the requirement to estimate the flux axis angle. This is done either by measuring the flux at two different points (with 90 degrees displacement), or estimating through rotor speed measurement (Ong, 1997). In this study, flux axis angle θ is calculated through rotor speed measurement:

$$\theta = \int \omega \, dt = \int \left(\omega_r + \frac{x_m}{T_r} \frac{i_{qs}}{\lambda_{dr}} \right) dt \tag{13}$$

The wind turbine converter is designed to control the rotational speed in order to produce the maximum output power, where the indirect vector control is used. The control part consists of a speed controller and the d-q current controllers. The d-axis current component is generally set to maintain the rated field flux in the whole range of speed, while the speed loop will generate the q-axis current component through a PI controller to control the generator torque and speed at different wind speed as shown in Fig. 3.

The proportional and integral gains for speed controller used in simulation are $K_p = 12$ and $K_i = 25$ respectively.

Shunt inverter of UPQC: The shunt inverter described in this paper has two major functions. First, to compensate the current harmonics generated by the nonlinear load and reactive power and to inject the active power of WECS to grid (Normal Mode). Second, to supply the power to the load when the voltage interruption occurs in the source side (Interruption Mode). Figure 4 shows the controller developed for the shunt compensator.

Normal mode operation: The measured load current is transformed into synchronous d-q reference frame with the sine and cosine functions calculated using a PLL (Phase Locked Loop) (Hu and Chen, 2000):

$$i_{ldq0} = T_{abc}^{dq0} \, i_{abc} \tag{14}$$

$$T_{abc}^{dq0} = \frac{2}{3} \begin{bmatrix} \cos\theta & \cos\left(\theta - \frac{2\pi}{3}\right) & \cos\left(\theta + \frac{2\pi}{3}\right) \\ \sin(\theta) & \sin\left(\theta - \frac{2\pi}{3}\right) & \sin\left(\theta - \frac{2\pi}{3}\right) \\ \frac{1}{2} & \frac{1}{2} & \frac{1}{2} \end{bmatrix} \tag{15}$$

with this transformation, the fundamental positive sequence components are transformed into dc quantities in d and q axes, which can easily be extracted by Low-Pass Filter (LPF). All harmonic components are transformed into ac quantities with a fundamental frequency shift:

$$i_{ld} = \bar{i}_{ld} + \tilde{i}_{ld} \, , \, i_{lq} = \bar{i}_{lq} + \tilde{i}_{ld} \tag{16}$$

which

$$i_l = i_s + i_c \tag{17}$$

where, i_l is the nonlinear load current, i_s is the source current and i_c is compensating current.

The switching loss can cause the dc link capacitor voltage to decrease. Other disturbances, such as unbalances and sudden variations of loads can also cause this voltage to fluctuate. In order to avoid this, in Fig. 3a PI controller is used.

To avoid dc voltage fluctuation, a PI controller is used. The input of the PI controller is the error between the actual capacitor voltage and the desired value, its output Δi_{dc} is then added to the reference current component in the d-axis to form a new reference current:

$$i_{cd}^{*} = \tilde{i}_{ld} + \Delta i_{dc} \, , \, i_{cq}^{*} = i_{lq} \tag{18}$$

When the dc link voltage decreases from desired value, the shunt inverter draws active power from grid to regulate its voltage. When WECS injects power to dc link, the bus voltage increases, in this case, the shunt inverter injects power to grid to maintain dc link voltage at nominal value. The proportional and integral gains for dc voltage controller used in simulation are $K_P = 0.5$ and $K_I = 0.05$, respectively.

As shown in Fig. 5, these reference currents in (18) are then inversely transformed into a-b-c reference frame. And the output compensatory currents of the shunt compensator are obtained by a PWM voltage current control.

Interruption mode operation: By estimating the entering voltage and current from the both ends of Solid-state Breaker (SSB) terminals as input signals, if the interruption exceeds a threshold level, then the SSB is opened into the islanding mode. Hereafter if the disturbances are removed, the SSB is closed immediately into normal mode.

When the voltage interruption occurs and SSB opens, the WECS provides the active power to maintain the load voltage constant. The shunt inverter starts to perform the voltage and current control using the PI controller. Figure 5 shows the voltage control block diagram of shunt inverter in interruption mode (Han *et al*., 2006).

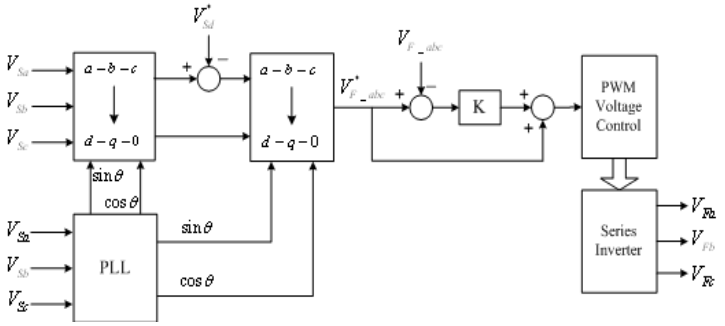

Fig. 6: Control block diagram of the shunt converter of the UPQC

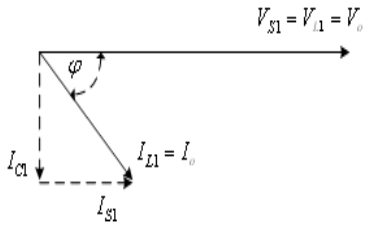

Fig. 7: Phasor diagram of shunt inverter of UPQC

Series inverter of UPQC: The function of series inverter is to compensate the voltage disturbance in the source side, which is due to the fault in the distribution line. The series inverter control calculates the reference value to be injected by the series inverter as shown is Fig. 6.

The system voltages are detected and then transformed into synchronous d-q-0 reference frame using (19) (Basu *et al*., 2007):

$$V_{sdq0} = T_{abc}^{dq0} V_{sabc} \tag{19}$$

The load bus voltage should be kept sinusoidal with constant amplitude even if the voltage on system side is disturbed. So the expected load bus voltage in d-q-o reference frame has only one value

$$V^*_{idqo} = T_{abc}^{dq0}.V^*_{labc} = \begin{bmatrix} V_m \\ 0 \\ 0 \end{bmatrix} \tag{20}$$

where,

$$V^*_{labc} = \begin{bmatrix} V_m \cos(\omega t + \theta) \\ V_m \cos(\omega t + \theta - 120^o) \\ V_m \cos(\omega t + \theta + 120^o) \end{bmatrix} \tag{21}$$

where, V_m is peak value of desired load voltage, and θ is phase angle of load voltage which is determined by PLL (Phase Locked-Loop). This means d-axis of load reference voltage equals V_m while q-axis and zero axis of load reference voltage equals zero.

The compensation reference voltage is:

$$V^*_{fdqo} = V^*_{ldqo} - V_{sdqo} \tag{22}$$

The compensation reference voltage in (22) is then inversely transformed into a-b-c reference frame. Comparing the compensation reference voltage with a triangular wave, the output compensation voltage of the series compensator can be obtained by PWM voltage control.

Phasor diagram of UPQC: Figure 7 shows phasor diagram of shunt inverter of UPQC for fundamental power frequency when the supply voltage equals the desired load voltage (Basu *et al*., 2007).

When the supply voltage has no deficiency; $V_S = V_{L1} = V_{S1} = V_o$ (a constant), and the series injected voltage V_{inj} requirement is zero. This state is represented by adding suffix "1" to all the voltage and current quantities of interest. The load current is I_{L1} ($I_{L1} = I_L$) and the shunt inverter compensates the reactive component I_C of the load, resulting in unity input power factor. Thus, the current drawn by the shunt inverter is $-I_{C1}$, which is opposite to the load reactive current I_{C1}. As a result, the load always draws the in-phase component I_{s1} from the supply. For non-linear loads, the shunt inverter not only supplies the reactive current, but also the harmonic currents required for the load. Thus, after the compensation action of the shunt inverter, only the fundamental active component of the current is required to be supplied from the utility.

Figure 8 shows phasor diagram of shunt and series inverter of UPQC for fundamental power frequency when the supply voltage sags and UPQC injects V_{inj} to maintain the load voltage at its desired level (Basu *et al*., 2007).

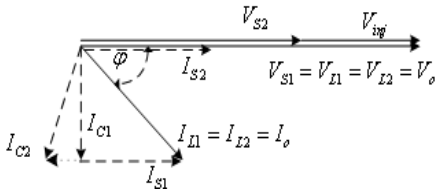

Fig. 8: Phasor diagram of shunt and series inverter of UPQC

As soon as the load voltage V_L sags, the UPQC is required to take action to compensate for the sag, so that V_L is restored to its desired magnitude.

This condition is represented by adding suffix "2" to the parameters. Consequently the load current changes to I_{L2}. The shunt inverter injects I_{C2} in such a way that the active power requirement of the load is only drawn from the utility. Therefore, from the utility side the load power factor is always unity. It can be observed from the phasor diagram that the utility current is I_{S2}, and is in phase withV_{S2}.

If the active power demand is constant:

$$V_{S1}\, I_{S1} = V_{S2}\, I_{S2} \tag{23}$$

which can be written as:

$$I_{S2} = \frac{V_{S1}\, I_{S1}}{V_{S2}} \tag{24}$$

VA rating calculation of shunt and series inverter: Volt Ampere (VA) rating of series and shunt inverters of UPQC determines the size of the UPQC. The power loss is also related to the VA loading of the UPQC. Here, the loading calculation of shunt and series inverters of UPQC with presence of DG at its dc link has been carried out on the basis of linear load for fundamental frequency.

The load voltage is to be kept constant at V_o p.u. irrespective of the supply voltage variation:

$$V_S = V_{L1} = V_{L2} = V_{S1} = V_o \; p.u \tag{25}$$

The load current is assumed to be constant at the rated value:

$$I_L = I_{L1} = I_{L2} = I_o \; p.u \tag{26}$$

Assuming the UPQC to be lossless, the active power demand in the load remains constant and is drawn from the source:

$$V_S I_S = V_{\ L} I_L \cos\varphi \tag{27}$$

In case of a sag when $V_{S\,2}\, V_{1S}$, where x denotes the p.u. sag:

$$V_{S2} = (1-x)V_{S1} = V_o\,(1-x)\; p.u. \tag{28}$$

to maintain constant active power under the voltage sag condition as explained in (1):

$$I_{S2} = \frac{V_{S1} I_L \cos\varphi}{V_{S1}\,(1-x)} = \frac{I_o \cos\varphi}{1-x}\; p.u. \tag{29}$$

therefore series inverter VA rating equals to:

$$S_{seinv.} = V_{inj}\; I_{s2} = \frac{V_o I_o\,(x\cos\varphi)}{1-x}\; p.u. \tag{30}$$

Injected current through shunt inverter is:

$$I_{C2} = \sqrt{I_{LI}^2 + I_{S2}^2 - 2I_{LI} I_{S2}\cos\varphi} = I_o \frac{\sqrt{(1-x)^2 + \cos^2\varphi\{1-2(1-x)\}}}{1-x} \tag{31}$$

therefore shunt inverter VA rating equals to

$$S_{shinv.} = V_o I_o \frac{1}{1-x}\sqrt{(1-x)^2 + \cos^2\varphi\{1-2(1-x)\}} + I_o^2 \frac{(1-x)^2 + \cos\varphi\{1-2(1-x)\}}{(1-x)^2} Z_{shinv}.p.u. \tag{32}$$

Figure 9-10 show VA loading of series and shunt inverters of UPQC for a wide range of power factor and supply voltage sag variations. The VA loading of inverters is calculated for Occurrence of supply voltage sag from 10 to 50% and power factor variations from 0.6 lagging to unity power factor, with $Z_{sh} = 1_{pu}$ in all cases. The range of supply voltage sag has been chosen such that most practical cases are observed to be in this range as available from power quality survey reports.

Effect of connecting DG to UPQC on UPQC converters VA: By connecting DG to the DC link of UPQC, the active power required by series inverter can be supplied from DG. Hence, the freed capacity created on the shunt inverter can be used for active power flow (transmission) to grid. These capacities of inverters are detailed as follows:

From Fig. 8 one can deduce that the current in shunt inverter which compensates voltage drop in dc link due to operation of series inverter, is parallel with I_{S1} whose vector sum with I_{C1} will yield I_{C2}. That would be active

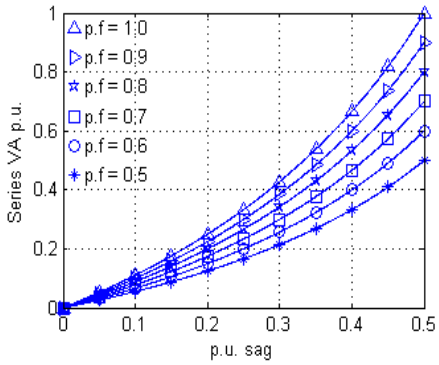

Fig. 9: VA loading of series inverter of UPQC for different power factor and p.u voltage sag values

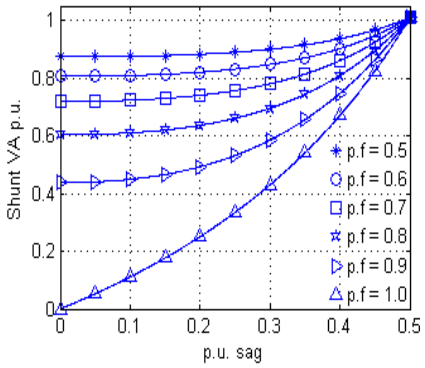

Fig. 10: VA loading of shunt inverter of UPQC for different power factor and p.u voltage sag values

Table 1: P.u active current flow in shunt inverter for series compensation for various cos φ and voltage sags

p.u sag/cos φ	0.1	0.2	0.3	0.4	0.5
0.5	0.055	0.125	0.213	0.333	0.50
0.6	0.066	0.15	0.255	0.40	0.60
0.7	0.077	0.175	0.30	0.533	0.80
0.8	0.088	0.20	0.342	0.533	0.8
0.9	0.099	0.225	0.385	0.60	0.90
1.0	0.11	0.25	0.428	0.667	1.00

Table 2: Capability of shunt inverter to transmission of active and reactive current for different power factors

cos φ	0.50	0.6	0.70	0.8	0.90	1.0
I_{C1}	0.86	0.8	0.71	0.6	0.43	0.0
I_{DG-C2}	0.50	0.6	0.70	0.8	0.90	1.0

current in the direction of I_{S1} and its rms value is I_{SE-C2} which is equal to vector difference of I_{C1} and I_{C2}.

$$I_{SE-C2} = \sqrt{I_{C2}^2 - I_{C1}^2} \tag{33}$$

From Fig. 8 it can be found that:

$$I_{C1} = I_o \sin\varphi \tag{34}$$

By substituting I_{C1} and I_{C2} from (34) and (31) respectively, I_{SE-C2} is equals to:

$$I_{SE\_C2}^2 = I_o^2 \frac{(1-x)^2 + \cos^2\varphi\{1-2(1-x)\}}{(1-x)^2} - I_o^2 \sin^2\varphi \tag{35}$$

Simplifying (35) results in:

$$I_{SE-C2} = I_o \frac{x\cos\varphi}{1-x}\, p.u. \tag{36}$$

Assuming, $I_o = 1_{pu}$ the value of I_{SE-C2} will be given for different values of load power factor. Table 1 demonstrates the perunit active current in the shunt inverter for series compensation for different power factors and voltage sag values. By installing DG on dc link of UPQC and supplying active power required for series compensation by DG, the active power of DG can flow to grid through shunt inverter.

Assuming shunt inverter design of 1 p.u capacity for complete current compensation and voltage sag compensation up to 0.5 p.u, by connecting DG to the UPQC dc link, 1 p.u shunt inverter will be able to flow 1 p.u current of DG to grid. Table 2 shows the possible capacity of shunt inverter for carrying Dg active current for different power factor values. Therefore the proposed configuration is capable of DG active power transmission of 1 p.u to thr grid without any change in the capacity of series and shunt inverters.

Economic analysis of linking DG with UPQC: In this section, the economic analysis of separate linking of UPQC and DG to distribution network by combined scheme (as discussed in this study) is carried out and compared. In the combined operation of UPQC and DG, an inverter is used less compared to the separate operation of them. On the other hand, there is no need for DG converter and its duty is done by shunt inverter. The shunt inverter transmits the active power of DG to grid besides compensating the reactive power and harmonics of load current without increase of shunt inverter rating.

The investment cost of inverter IC_{elec} can be expressed as (Kaldellis and Kavadias, 2007):

$$IC_{elec} = \lambda N_P^{1-\tau}$$
$$\lambda = 483(\$/kW) \tag{37}$$
$$\tau = 0.083$$

Table 3: Comparison of investment cost and economic saving of separate and combined UPQC and wind energy system

Rating/	15 KVA		150 KVA		1500 KVA	
Equipment	Separate	Combined	Separate	Combined	Separate	Combined
Wind turbine	10515	10515	105004	105004	1050000	1050000
PWM rectifier	5786	5786	47800	47800	39484	1394841
Grid side inverter	5786	-	47800	-	394841	-
Shunt inverter	5786	5786	47800	47800	394841	394841
Series inverter	5786	5786	47800	47800	394841	394841
Whole	33662	27876	296202	248702	2629366	2234525
Economic saving	20.7%	19.1%	17.6%			

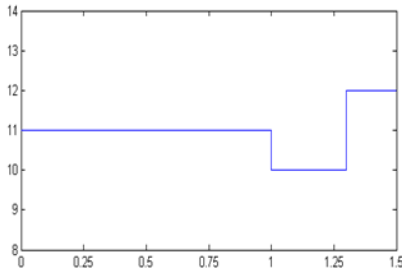

Fig. 11: Simulated wind model (m/s) for wind speed variations step

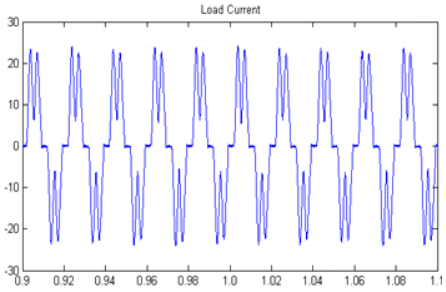

Fig. 12: Load current (A)

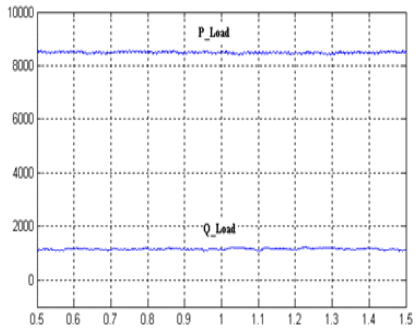

Fig. 13: Active and reactive power consumed by load

which N_p is the rated power of inverter. Since UPQC has two inverters, the investment cost of UPQC is same as two inverters. The investment cost of wind turbine by rated power of N_{WT}, can be demonstrated by (Kaldellis and Kavadias, 2007):

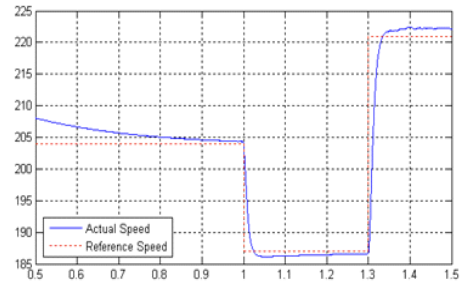

Fig. 14: Reference and actual rotor speed in rad / s

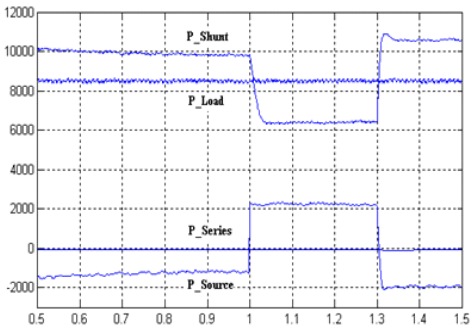

Fig. 15: Injected active power by source and series and shunt inverters of UPQC and consumed power of load

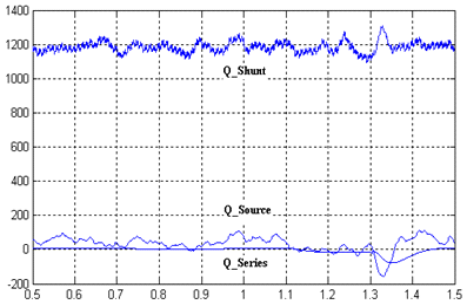

Fig. 16: Injected reactive power by source and series and shunt inverters of UPQC

$$IC_{WT} = \left(\frac{a}{b + N_{WT}^{x}} + c \right) N_{WT}$$

$$a = 8.7 \times 105(\$ / kW)$$
$$b = 621$$
$$c = 700(\$ / kW) \quad (38)$$
$$x = 2.05$$

Using (37) and (38), the investment cost of separate UPQC and WECS and also combined UPQC and WECS can be estimated. Table 3 shows investment costs of separate and combined configurations for three different ratings. Economic savings due to using combined configuration compared to separate UPQC and WECS can be seen in Table 3. These results show the proposed configuration has 17.6% up to 20.7% economic saving depending on different ratings.

RESULTS AND DISCUSSION

In order to inspect different variables, analysis will be carried out of different parameters in three steps. First, the wind speed variation is considered and the way to inject power to the grid is studied. Second, voltage sag of 100v in peak at a constant wind speed is applied and the results are studied. Finally, interruption is applied and the corresponding power injection to load is observed.

Wind speed variations: The wind model used in the simulation consists of base component that is a constant speed and a gust component for fast variations in wind speed (Kim and Kim, 2007). The simulated wind model is shown in Fig. 11.

The applied load is an RC load with uncontrolled diode rectifier with a THD of more than 40%. The load current is shown in Fig. 12. In Fig. 13 the active and reactive power consumed by the load are demonstrated.

As was described in the previous section, the optimal rotor speed to maximize the output power of wind turbine in different wind speeds, is obtained by adjusting tip speed ratio (λ) at its optimal value. This is applied as the generator's reference speed so that the wind turbine rotates with such speeds that maximize the output power for different wind speeds. Figure 14 shows the reference and actual rotor speed in $^{rad/s}$. As is evident, the generator tracks the reference speed (or the optimal speed to gain the highest output power) after getting past the starting stage.

In Fig. 15 the injected active power by series and shunt inverters of UPQC, source side and power consumption of load are shown. The load power consumption should equal the sum of injected power by source, series and shunt inverters at each moment. As is obvious in the figure, until t = 1s, the wind speed is at its rated value and the injected active power by shunt converter is ^{10KW}. Since the power required by the load is 8.5 kW, the surplus wind system power is injected into the grid and the power flow direction in grid is reversed. Therefore, the source power is negative within this interval. By the wind speed decreasing from t = 1 s till t = 1.3 s, the active power injected by the shunt inverter into the grid is decreased and part of the load power is supplied from the source. At time t = 1.3s, the wind speed exceeds the nominal value and the injected power through shunt inverter exceeds^{10K}. In Fig. 15 it is seen that the change in wind speed has no effect on the performance of series inverter and it does not inject or receive any power. The series inverter begins to operate when any voltage disturbances occur.

The reactive power injected by the source, series and shunt inverters of UPQC is illustrated in Fig. 16. The reactive power injected by shunt inverter is consumed by the load. Hence the grid capacity is not dedicated to reactive power support and the source reactive power became nearly zero. Since the source voltage has no disturbance, the reactive power of series inverter also remains zero.

The current direction is reversed at the instances t = 1 s and t = 1.3 s. In other words, within the time interval t = 1 s to t = 1.3 s, the source receives power from the wind system (Fig. 17).

Figure 18 shows dc link voltage of UPQC. At the initial moments, the startup of induction generator necessitates reactive power absorption which is supplied via dc link capacitor and this causes dc link capacitor's voltage drop. After startup of generator, the dc voltage remains so close to the reference voltage (780v). An abrupt change in wind speed, causes a change in the dc link voltage to some extent and gets back to the desired value after a short time.

Voltage sag: In this section, voltage sag at a given wind speed, 11m/s, is applied and the results are studied. A voltage sag with peak amplitude of 100v is applied from t = 1sec to t = 1.3sec. The source and load voltage are shown in Fig. 19. It is seen in this figure that the UPQC series inverter has modified load voltage correctly. In Fig. 20 the injected power by source and UPQC's inverters and also the consumed power by load are shown. The consumed power of load should be equal to the power injected by source and UPQC. As is shown, when the voltage sag occurs, the injected active power by shunt inverter is slightly decreased and the power injected by series inverter is increased by the same amount The source-injected power does not undergo any changes by the voltage sag.

Figure 21 shows reactive power injection by source and series and shunt inverters of UPQC. The reactive power required by load is supplied from the shunt

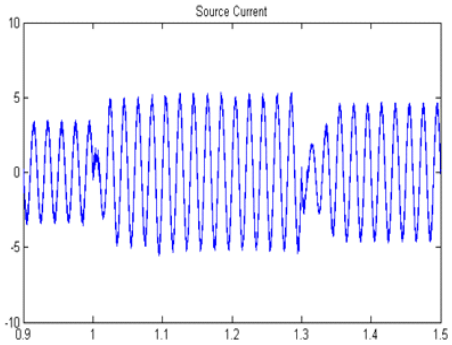

Fig. 17: Current drawn from the source

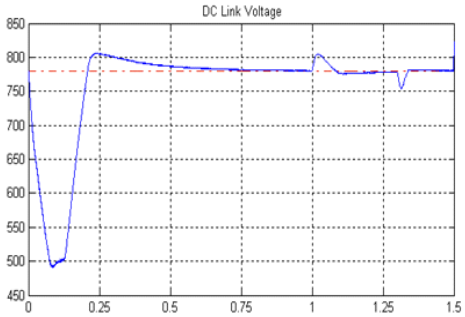

Fig. 18: DC link voltage of UPQC

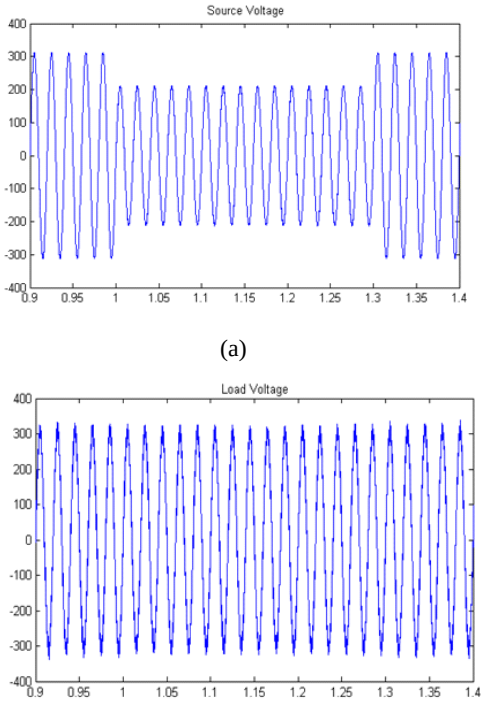

Fig. 19: Voltage sag compensation. (a) Source voltage. (b) Load voltage

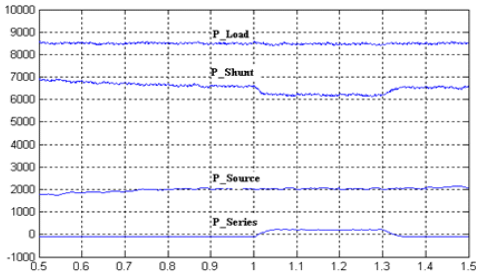

Fig. 20: Injected active power by source and series and shunt inverters of UPQC and consumed power of load

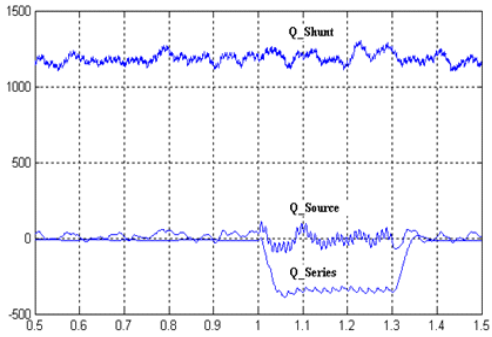

Fig. 21: Injected reactive power by source and series and shunt inverters of UPQC

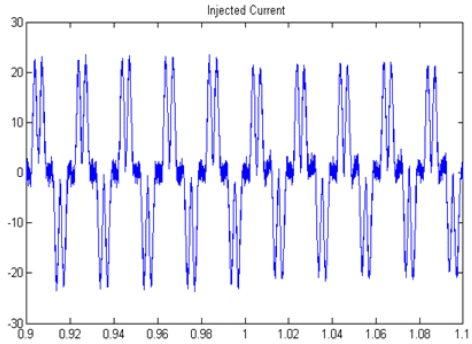

Fig. 22: Shunt inverter injected current during occurrence of voltage sag

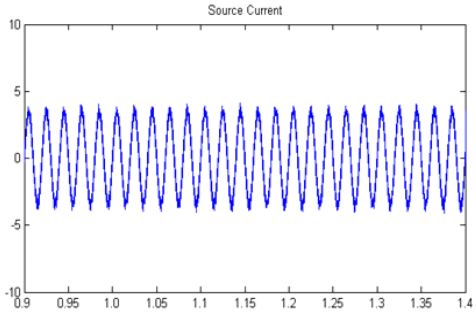

Fig. 23: Source current during occurrence of voltage sag

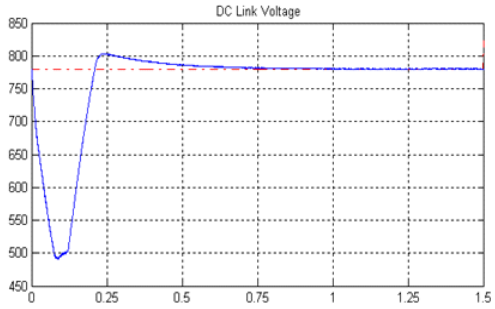

Fig. 24: DC link voltage of UPQC during occurrence of voltage sag

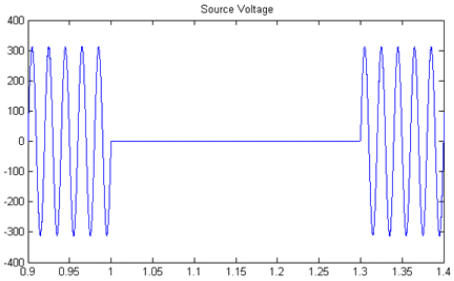

(a)

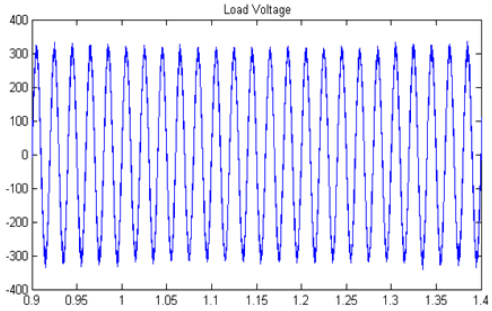

(b)

Fig. 25: Voltage interruption compensation. (a) Source voltage. (b) Load voltage

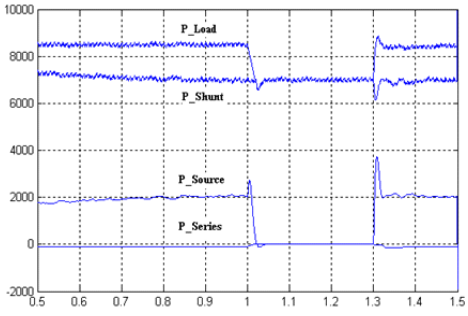

Fig. 26: Injected active power by source and series and shunt inverters of UPQC and consumed power of load during occurrence of voltage interruption

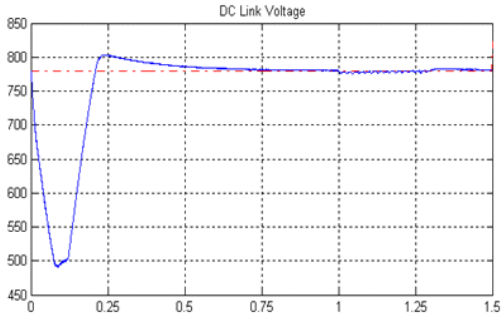

Fig. 27: DC link voltage of UPQC during occurrence of voltage interruption

inverter. Hence, the reactive power drawn from source will be zero. In normal operation, the series inverter does not inject or absorb any reactive power but it absorbs reactive power when the voltage is distored. Considering UPQC control circuit and values of d-q components of voltage, it is indicated that before voltage sag or disturbance, the q component of voltage is zero, while by the voltage sag; it will be changed and must be compensated. In order to compensate the load voltage when voltage sag occurs, the series inverter should inject active power and absorb reactive power.

The current in the shunt branch of UPQC is shown in Fig. 22. A significant percentage of load current is supplied through the shunt branch. In other words, the power generated by wind system is consumed by load. Hence, the current drawn from the source is negligible. Consequently, if the power generated by wind system is in excess of the load, the surplus power would flow into the grid (source). At the time t=1s, the current is slightly decreased. This is because of voltage sag and allocation of a part of wind system power to injection through series inverter to improve voltage sag.

The current drawn from the source is shown in Fig. 23. It is shown in this figure that the source current is sinusoidal and its amplitude is nearly 4A. The reason is the wind system function and active power injection through the shunt inverter. The harmonic current of load is supplied by shunt inverter and the source current remains sinusoidal. The dc link voltage is shown in Fig. 24. After startup of induction generator, the dc voltage value remains very close to the reference value. The voltage sag has no effect on dc link voltage, because the required power is supplied from the wind system. Hence the dc voltage will remain constant.

Voltage interruption: In this section, voltage interruption occurs from t = 1sec to t = 1.3sec at wind speed of 11m/s. As soon as the interruption occurs, SSB is opened and the shunt inverter control switches from grid-connected into islanding mode. Therefore the load and shunt inverter are isolated from grid. It is assumed that there is enough wind power to supply the load. In case the generated power of

wind system does not meet the required power of load, a part of load that has less importance, will not be supplied correspondingly.

Figure 25 shows the source and load voltage respectively. It is seen that after voltage interruption, load voltage is remained at its desired value due to shunt inverter operation.

The injected power of source, series and shunt inverters as well as consumed power of load is shown in Fig. 26. At each instant, the power consumed by load should be equal to the sum of injected powers. As is evident in the figure, as the outage occurs, the injected power by source and series inverter becomes zero and the wind system generated power is fed to the load through shunt inverter. As the outage is removed, SSB is closed and series inverter gets back to the circuit and also the shunt inverter control returns to grid-connected mod.

The dc link voltage is shown in Fig. 27. As is illustrated in the figure, the voltage control loop is functioning properly keeping dc link voltage level close to its reference value.

CONCLUSION

This study describes a combined operation of the unified power quality conditioner with wind power generation system considering investment cost. The proposed system can compensate voltage sag and swell, voltage interruption, harmonics, and reactive power in both interconnected mode and islanding mode. The speed of the induction generator is controlled according to the variation of the wind speed in order to produce the maximum output power. The VA rating of series and shunt inverters of UPQC are estimated for proposed system. The investment cost of proposed system is compared with investment cost of separated use of UPQC and WECS using the VA rating calculations and the economic saving due to use of proposed system is estimated nearly 20%. The performance of the proposed system was verified using computer simulations.

ACKNOWLEDGMENT

This research study has been financially supported by the office of vice chancellor for research of Islamic Azad University, Bushehr Branch.

REFERENCES

Abo-Khalil, A.G., H.G. Kim, D.C. Lee and J.K. Seok, 2004. Maximum output power control of wind generation system considering loss minimization of machines. IEEE 35th Annual Power Electron. Specialist Conference, 2: 1676-1681.

Akagi, H., Y. Kanazawa and A. Nabae, 2007. Instantaneous reactive power compensator comprising switching devices without energy storage components. IEEE Trans. Ind. Appl., 20: 625-630.

Aredes, M. and E.H. Watanabe, 1995. New control algorithms for series and shunt three-phase four wire active power Filters. IEEE Trans. Power Del., 10: 1649-1656.

Basu, M., P.D. Shyama and K.D. Gopal, 2007. Comparative evaluation of two models of UPQC for suitable interface to enhance power quality. J. Electr. Power Syst. Res., 77: 821-830.

Cavalcanti, M.C., G.M.S. Azevedo, B.A. Amaral and F.A.S., Neves, 2005. A photovoltaic generation system with unified power quality conditioner function. 31st Annual Conference of IEEE Industrial Electronics Society, pp: 1-6.

Datta, R. and V.T. Rangenathan, 2002. Variable-speed wind power generation using doubly fed wound rotor induction machine-a comparison with alternative schemes. IEEE Trans. Energ. Conv., 17: 414-421.

Datta, R. and V.T. Rangenathan, 2003. A method of tracking the peak power point for a variable speed wind energy conversion system. IEEE Trans. Energ. Conv., 18: 163-168.

Han, B., B. Bae, H. Kim and S. Baek, 2006. Combined Operation of Unified Power Quality Conditioner With Distributed Generation. IEEE Trans. Power Del., 21: 330-338.

Horiuchi, N. and T. Kawahito, 2001. Torque and power limitations of variable speed wind turbines using pitch control and generator power control. IEEE Power Eng. Soc. Summer Meet. 1: 638-643.

Hu, M. and H. Chen, 2000. Modeling and Controlling of Unified Power Quality Compensator. IEEE International Conference on Advances in Power System Control, Operation and Management, 2: 431-435.

Kaldellis, J.K. and K.A. Kavadias, 2007. Cost-benefit analysis of remote hybrid wind-diesel power stations: Case study Aegean Sea islands. J. Energ. Policy, 35: 1525-1538.

Karrari, M., W. Rosehart and O.P. Malik, 2005. Comprehensive control strategy for a variable speed cage machine wind generation unit. IEEE. Trans. Energ. Conver. 20(2): 415-423.

Kim, S. and E. Kim, 2007. PSCAD/EMTDC-based modeling and analysis of a gearless va variable speed wind turbine. IEEE Trans. Energ. Conver. 22(2): 421-430.

Ong, C.M., 1997. Dynamic Simulation of Electric Machinery, Using MATLAB and SIMULINK. 1st Edn., Upper Saddle River, Prentice-Hall.

Surgevil, T. and E. Akpınar, 2005. Modelling of a 5-kW wind energy conversion system with induction generator and comparison with experimental results. Renew. Energ. 30: 913-929.

Weisser, D. and R.S. Garcia, 2005. Instantaneous wind energy penetration in isolated electricity grids: Concepts and review. Renew. Energ. 30: 1299-1308.